International Journal Multidisciplinary
Homepage : https://journal.antispublisher.com/index.php/IJMI
Email : admin@antispublisher.com

e-ISSN : 3031-9870
IJMI, Vol. 3, No. 2, May 2026
Page 266-285

Experimental Study of Forced Convection Enhancement in a Porous Air Duct: Effects of Porosity and Particle Size

Mohammed Z. Hameed[1], Musa Mustafa Weis[2]
Northern Technical University, Iraq

DOI : https://doi.org/10.61796/ijmi.v3i2.456

Sections Info

Article history:
Submitted: November 17, 2025
Final Revised: December 31, 2025
Accepted: January 20, 2026
Published: February 16, 2026

Keywords:
Heat convection
Glass balls media
Fully open side and duct channel

ABSTRACT

Objective: *This research focuses on experimental studies of forced convection heat transfer in an air duct packed with a glass ball porous medium to enhance thermal efficiency and save energy.* ***Method:*** *Experiments were conducted with heat inputs of 100, 150, and 200 W and air velocities of 0.5, 0.75, and 1 m/s, while varying the ball diameter and porosity. Three electric tubular heaters fixed vertically were used for uniform heating.* ***Results:*** *The study shows that lower porosity media significantly increase heat transfer capability under the same airflow conditions. Glass balls with a porosity of 0.58 achieved a maximum enhancement, with increments of 66.10%, 89.79%, and 64.83% at 0.5 m/s for 100, 150, and 200 W, respectively. A strong linear relationship between Reynolds and Nusselt numbers was observed, with maximum Nusselt number enhancements of 72.92% and 24.61% at 0.5 and 0.75 m/s, respectively.* ***Novelty:*** *This study highlights the impact of glass ball size and porosity on heat transfer performance, demonstrating that smaller particles with higher porosity significantly improve thermal efficiency, though at the cost of increased flow resistance. The findings contribute valuable insights into optimizing porous media for energy-efficient heat transfer.*

INTRODUCTION

Experimental work is one of the fundamental components in thermal and engineering studies, as it enables the researcher to understand the actual behaviour of heat transfer and flow within complex systems. In this research, an experiment was designed and executed with the aim of improving heat transfer within a porous pad containing a porous medium of small glass beads. This chapter presents the adopted methodology, starting from the design of the experimental apparatus, followed by the materials and devices used, the measurement and calibration procedures, and finally, the computational aspects, which include the laws and equations employed to analyze the experimental results [1]. Previous studies have investigated heat transfer enhancement using porous media; however, several limitations can be identified. For instance, stainless steel balls with diameters ranging from 1 to 3 mm were used as a porous medium under Reynolds numbers between 3200 and 6500, with porosity values of 0.3690 and 0.3912 and applied heat fluxes of 6250 and 12,500 W/m². These studies were limited to a single porous material and did not explore alternative materials such as glass or aluminum, which may exhibit different thermo-hydraulic behaviors [2]. Other research demonstrated that viscous dissipation significantly influences heat transfer performance, particularly at higher Eckert numbers compared to Reynolds numbers, indicating additional heat generation within the porous medium. It was also reported that lower porosity intensifies this effect, thereby reducing heat transfer efficiency. Nevertheless,

such studies neglected the investigation of several influential parameters, including the impact of porosity under varying boundary conditions, and focused mainly on the assumption of local thermal non-equilibrium without addressing additional complexities encountered in practical applications [3]. Furthermore, some investigations analyzed heat transfer phenomena using two-dimensional models only, without extending the analysis to three-dimensional simulations. Since three-dimensional modeling provides a more realistic representation of flow and thermal fields, the absence of such analysis limits the applicability of the results. In addition, the effects of varying material properties, such as permeability and thermal conductivity, were not thoroughly examined [4]. Experimental studies on forced convection of water through vertical porous rings filled with glass spheres of different sizes and porosities have also been reported. However, these studies were restricted to liquid flow (water) and did not address air as a working fluid, nor did they incorporate numerical simulations to complement the experimental findings and enhance result validation [5]. In other works, although graphite porous media showed promising thermal performance, no comparative analysis was conducted against other advanced materials such as metal foams or composite structures. Additionally, variations in graphite properties arising during manufacturing, which may affect porosity and density, were not adequately considered [6]. Numerical investigations using COMSOL software have been carried out and validated against previous experimental data; however, such studies did not analyze the influence of different gap arrangements between porous elements or compare their effects on heat transfer performance. Moreover, they were limited to a single working fluid, overlooking the potential impact of using different fluids [7]. studies involving nanofluids as porous media in microchannels focused primarily on uniform heat flux conditions and did not consider variable heat flux scenarios. Furthermore, comparisons between different types of nanofluids were not conducted, and the role of porosity was not clearly addressed, leaving a significant research gap in understanding its influence on thermal performance.

RESEARCH METHOD

Fabrication of the Porous Pad

The purpose of the porous pad is to create an air space where the flow and temperature can be controlled, with the possibility of filling it with a porous medium made of small glass beads, as shown in figure (2-1). It was constructed from two interconnected chambers: a lower chamber (distribution chamber) in the shape of an inverted pyramid/triangle to distribute the flow, and an upper rectangular chamber open from the top to allow the hot flow to enter and exit.

The side walls were made of thick wooden panels (15 mm). Transparent plastic sheets (8 mm thick) were installed on the front and rear faces for easy visual monitoring. These panels were attached to the wooden sides using a CNC machine, and a thermal silicone material was used to achieve an airtight seal. Several holes were drilled on the plastic face to uniformly place the heaters on the thermal pad at four horizontal and three

vertical positions (4*3) with a diameter of 16 mm. Additionally, 3 mm diameter holes were distributed between the heaters to take precise readings inside the pad.

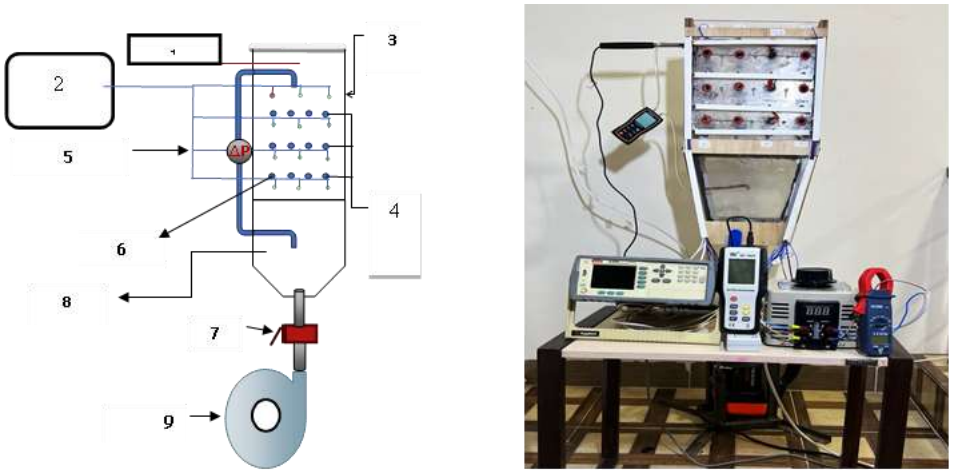

Figure (2-1) is a schematic diagram of a device with the photographic image used in this study.

Where: 1) Hot wire (velocity measurement), 2) Wood frame, 3) Data logger, 4) Voltage, 5) Thermocouple, 6) Heat pipe hole, 7) Ball valve, 8) Plastic and 9) Fan

Heat Pipe design

The heat pipe was fabricated in accordance with the design of the porous pad. A tubular heating element with a length of 17 cm and a diameter of (1.5875 cm) was used for this purpose. It operates with a variable voltage ranging from 0 to 220 volts, with a resistance of 241 ohms. This heating element was designed to be the primary source of heat generation. It works by passing an electric current through a resistance wire surrounded by a metal tube, allowing direct and safe heat transfer to the surrounding medium.

The heating element was placed inside a copper tube with a length of 15 cm and a diameter of 0.962 cm. The space between the heating element and the copper tube was filled with glass powder (prepared by grinding glass using a grinding machine) to ensure the stability of the heater inside the tube and to enhance the distribution of heat towards the surrounding medium. The end of the tube was sealed with tin, while the other end (containing the wire exit) was sealed with thermal silicone.

For measuring the temperature distribution around the heat pipe, four thermocouples of type (T) were fixed inside the body of the tube at angles of 0°, 90°, 180°, and 270° through four dedicated holes in the tube. Each thermocouple was covered with a special thermal insulation material to protect the wires from damage or burning due to the high temperatures. The figure (2-2) below illustrates the fabrication of the heat pipe.

Figure (2-2) illustrates the manufacturing details of the thermal tube

Temperature Measurement System

To record the temperatures inside the porous pad, thermocouples of type (T) are distributed systematically at the test section in a regular arrangement (3 rows × 4 columns), covering the length, width, and height of the pad. The sensors are mounted on thin supports that are as thermally non-conductive as possible (such as thin plastic tubes) to minimize airflow disturbance inside the pad.

All sensors are connected to a data logger system, with a total of 12 thermocouples of type (K) distributed inside the pad. Additionally, 12 thermocouples are placed in the heaters pipe to monitor the temperature in relation to the heat generation. This setup ensures precise temperature measurement throughout the system, allowing for comprehensive analysis of the heat distribution within the porous pad.

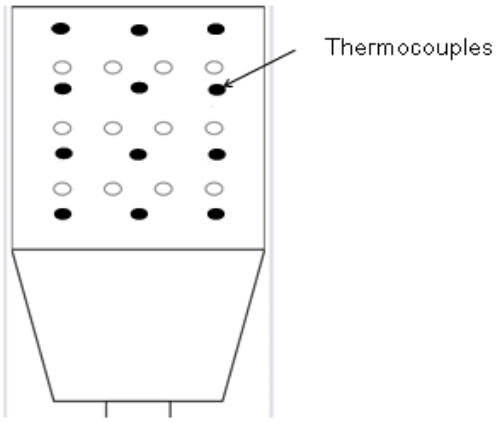

Figure (2–3) shows the locations of the thermocouples on

Air Velocity and Pressure Difference Measurement System

A Hot Wire Anemometer as shown in (2-4) was used to measure air velocity within the porous pad, inflated by an electric blower. This device operates by heating a very thin wire, whose temperature decreases when exposed to airflow. The temperature change is converted into a digital value representing air velocity, particularly accurate at low speeds. A flexible tube was connected from the top of the pad to the sensor, ensuring

direct air flow measurement. Additionally, A figure (2-5) show a digital manometer (SNDWAY SW-512C) was used to measure pressure difference within the pad. The manometer was connected to the lower and upper ports of the pad, measuring the pressure difference (ΔP = P1 - P2) and displaying it on the screen. This setup provides precise data on air velocity and pressure distribution for performance analysis.

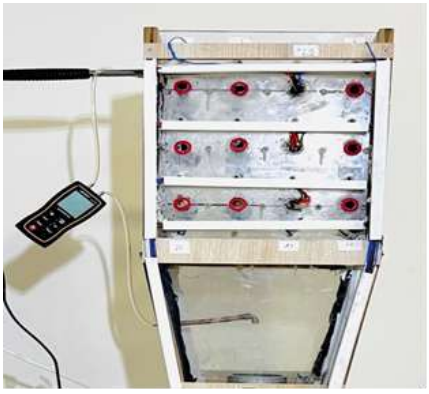

Figure (2-5) shows a manometer on the air

Figure (2-4) is a picture of an air velocity air pad

Mathematical modules

This chapter explains the fundamental equations for the thermal performance of a porous media filled with glass beads when the air passing through it is heated. This is based on the application of convection heat transfer equations in two cases: first, when the air flows without a porous medium, and second, when the porous medium is present within the air cushion. The chapter also addresses finding the relationships between dimensionless quantities (such as Nussle's number, Reynolds' number, and pressure differential) and determining the efficiency of the porous medium containing the glass beads. This is achieved using a mathematical model representing the porous cushion under consideration.

Porous media

The porosity of the porous medium (PM) is influenced by the diameter of the glass spheres and the hydraulic diameter of the test section. It is calculated using the following equation: [8], [9].

Where

V_T is the volume of the channel containing the porous medium (PM) (m^3), Vp is the volume of the porous medium (m^3), A_c is the cross-sectional area of the channel (test section) (m^2), L is length of test section and V_{Tb} is a volume of total porous media.

Thermal conductivity and density

The thermal conductivity of the porous medium (PM), consisting of glass spheres, is 0.78 W/m·K, and the density is 2700 kg/m^3[10]. to find thermal conductivity effect we use[11, 12]

$$K_m = K_f\{1 - \sqrt{(1-\varepsilon)} + \frac{2\sqrt{(1-\varepsilon)}}{1-\lambda\beta} \times \left[\frac{(1-\lambda)\beta}{(1-\lambda\beta)^2} \ln\left(\frac{1}{\beta\lambda}\right) - \frac{\beta-1}{2} - \frac{\beta-1}{1-\lambda\lambda}\right.$$

Where

$\beta = 1.25\{\frac{1-\varepsilon}{\varepsilon}\}^{\frac{10}{9}}$ and $\lambda = \frac{k_f}{k_s}$

And for density

$\rho_b = \frac{M_b}{V_{Tb}}$

Calculation of D_H

When using porous materials, we calculate the hydraulic diameter of the glass beads (D_{Hb}) using the following equation:

$$D_{Hb} = \frac{2d_P\varepsilon}{3(1-\varepsilon)}$$

Where dp is diameter of glass (16 mm and 25 mm)

To find the property of air in the air pad we depending on the average air temperature through test section [13]

$$T_m = \sum T_{air\ m}/12$$

The property in this experimental including (ρ , k , cp &μ
We depending on the heat transfer book by yunus cengile

To calculating heat transfer through the air pad we calculate the average input air temperature and outlet air temperature [14]

$$T_{in} = \sum T_{air\ in}/3$$

$$T_{out} = \sum T_{air\ out}/3$$

And heat transfer formula is used in air pad

$$Q_T = \dot{m} \times cp \times (T_{out} - T_{in})$$

4- Air flow mass ($\dot{m}$) is find in the test section find by

$$\dot{m} = \rho \times u_\infty \times A_T$$

Where cross section of pad A_T is find as a :

$$A_T = W \times L$$

To analyze the calculation of airflow through a set of pipes arranged in a matrix [15]

$$u_m = \frac{u_\infty (\frac{Sn}{2})}{(\frac{Sn}{2})^2 + Sp^2)^{0.5} - d}$$

Where

Sp: represents the distance between the centers of two tubes in a horizontal position.

Sn: represents the distance between the centers of two tubes in a vertical position.

u_∞: represents the air velocity passing through the air cushion.

u_m: represents the average air velocity through the tubes arranged in a regular pattern.

5- we find the Reynolds number in the case of an empty (without a porous medium).:

$$Re = \frac{\rho_f u_m D_H}{\mu_f}$$

Where

$$u_p = \frac{u}{\varepsilon}$$

When porous materials are added to the test section , the Reynolds number can be calculated using the equation.[16]

$$Re_p = \frac{\rho_f u_\varepsilon D_{Hb}}{\mu_f}$$

$$where$$

$$u_p = \frac{u}{\varepsilon}$$

And to find D_h in the porous media we use :

$$D_{Hb} = \frac{2d_b\varepsilon}{3(1-\varepsilon)}$$

Where d_b is a glass balls diameter

6- Heat transfer coefficient for each heaters a ra find as a :[17]

$$h_{ave} = \frac{Qt/3}{A_s(T_s - T_{m\,sur})}$$

Where A_s is find as

$$A_s = \pi D_t L_t$$

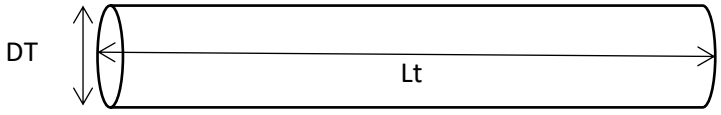

Fig (3-1) show dimension of heat pipe

For each heat pipe element T_s

$$T_s = \frac{\sum T_{se}}{4}$$

And for local heat transfer coefficient in the heat element are find in four position :

$$h_\theta = \frac{Qt/3}{A_s(T_{s\theta} - T_{sur})}$$

4- To find average Nu in each heat pipe we use :[18]

$$Nu_{ave} = \frac{h_{ave} \times D_h}{k_m}$$

And for local Nu we find in the heat pipe position :

$$Nu_{loc} = \frac{h_\theta \times D_h}{k_m}$$

5- We use a manometer to measure the pressure difference as air enters and exits the air pads.

the permeability is calculated based on the diameter and porosity of the spheres using the following equation [19]

$$K = \frac{\varepsilon^3 d_p^2}{175(1-\varepsilon)^2}$$

RESULTS AND DISCUSSION

This section presents a detailed analysis of the experimental results obtained from the forced convection of air through a porous pad filled with glass beads. The effects of airflow velocity, heat input, particle size, and porosity on the thermo-hydraulic performance of the system are discussed in terms of temperature distribution, Nusselt number, Reynolds number, and pressure drop. The results are interpreted based on the underlying physical mechanisms governing heat transfer and fluid flow in porous media.

Effect of temperature distribution on the surface of the heat pipe

The temperature distribution around the heat pipe surface was measured at four angular positions (0°, 90°, 180°, and 270°) for different airflow velocities and heat inputs. Figures (4-1) & (4-2) The results indicate a clear non-uniform temperature distribution along the circumferential direction of the heat pipe.

For the lowest airflow velocity (0.5 m/s), as shown in figure (4-3)the surface temperatures were relatively high due to weaker convective cooling. The maximum temperatures were consistently observed at the 90° position, which can be attributed to reduced direct airflow impingement on this region. In contrast, the lowest temperatures occurred at the 270° position, where the airflow first contacts the heat pipe surface, resulting in enhanced convective heat transfer.

In figure (4-4)shown the porous medium was introduced, a significant reduction in surface temperature was observed at all angular positions. This behavior is primarily due to the increased effective thermal conductivity of the medium and the disruption of the thermal boundary layer caused by the presence of the glass beads. The porous structure enhances mixing and increases the heat transfer surface area, thereby promoting stronger heat exchange between the solid surfaces and the flowing air.

Increasing the airflow velocity from 0.5 to 1 m/s led to a more uniform temperature distribution around the heat pipe. Higher velocities reduce thermal resistance by thinning the boundary layer and increasing turbulence intensity within the porous structure. Similar trends were observed when increasing the heat input from 100 W to 200 W, although higher heat flux resulted in elevated surface temperatures due to the increased thermal load.

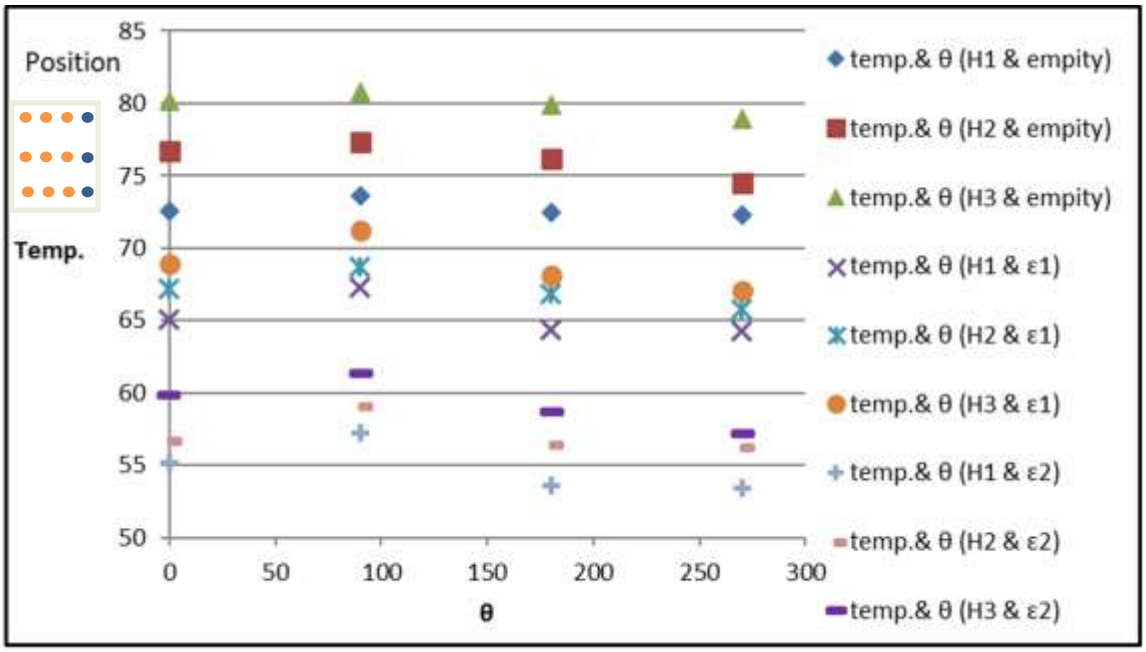

Figure (4-1) the effect of temperature angle at P1 & V1

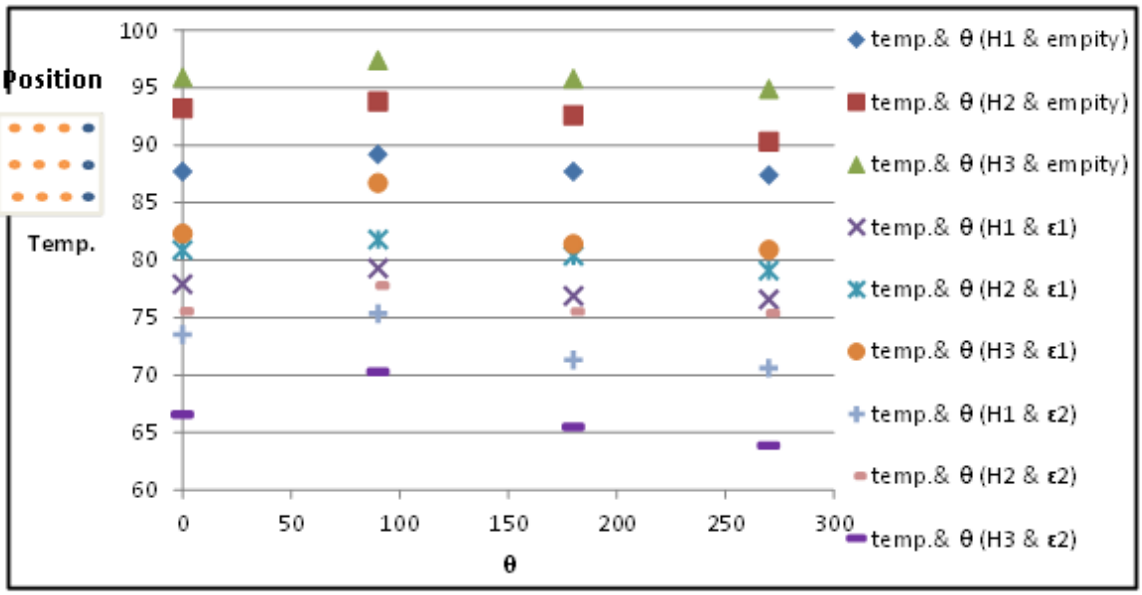

Figure (4-2) the effect of temperature angle at P2 & V2

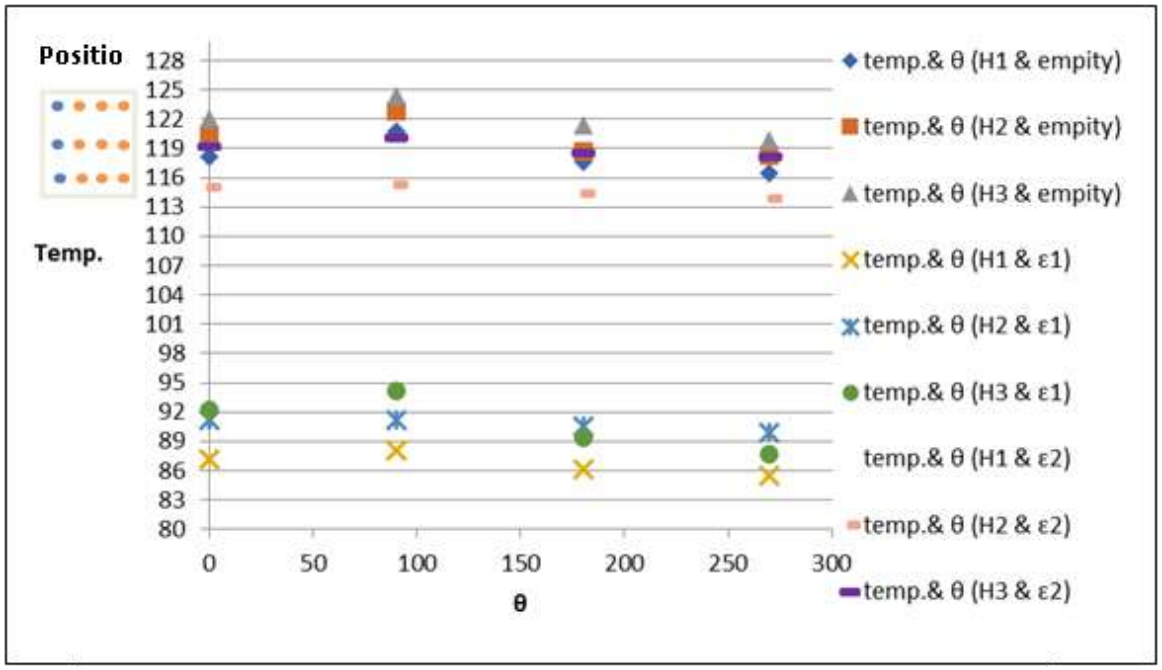

Figure (4-3) the effect of temperature angle at P1& V3

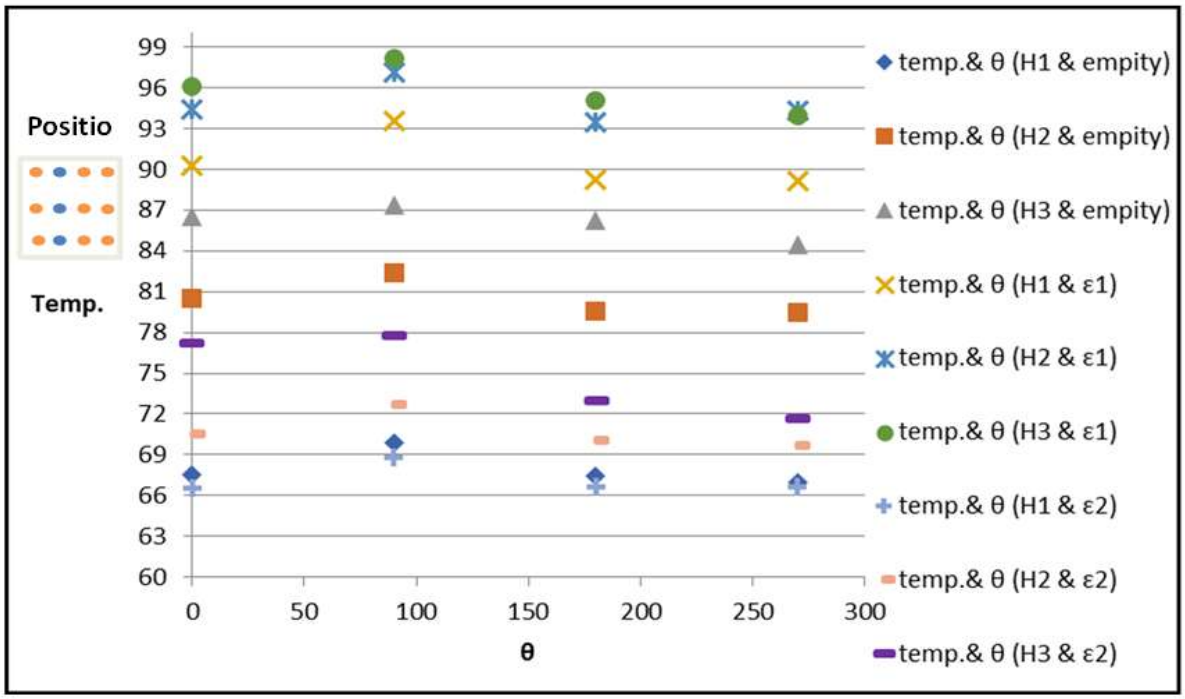

Figure (4-4) the effect of temperature angle at P1 & V3

Relationship between the average Nusselt number and the Reynolds number

The relationship between the average Nusselt number (Nu) and Reynolds number (Re) is illustrated in figure (4-5) to (4-7) for both porous and non-porous configurations. In all cases, Nu increased monotonically with Re, indicating enhanced convective heat transfer at higher flow rates. In the absence of porous media, the increase in Nu with Re was relatively modest due to the limited heat transfer area and stable boundary layer development. However, when glass balls were introduced, a substantial enhancement in

Nu was observed. This improvement is attributed to several mechanisms, including increased surface area, repeated boundary layer interruption, and flow acceleration through the interstitial spaces between particles. High glass balls produced higher Nusselt numbers compared to larger beads under identical operating conditions. This is mainly due to their high hydraulic diameter and higher specific surface area, which intensify heat exchange between the solid matrix and the fluid. Nevertheless, the enhancement in Nu was accompanied by an increase in pressure drop, highlighting the importance of considering thermo-hydraulic performance rather than heat transfer alone.

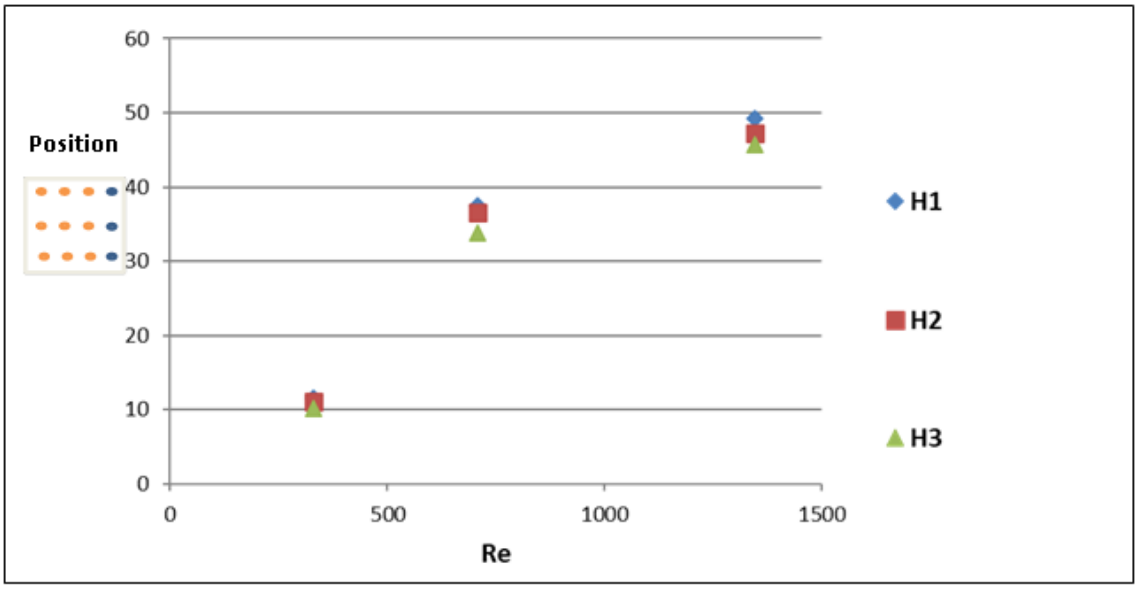

Figure (4–5) shows the relationship between Nu and Re in the P1 & V3

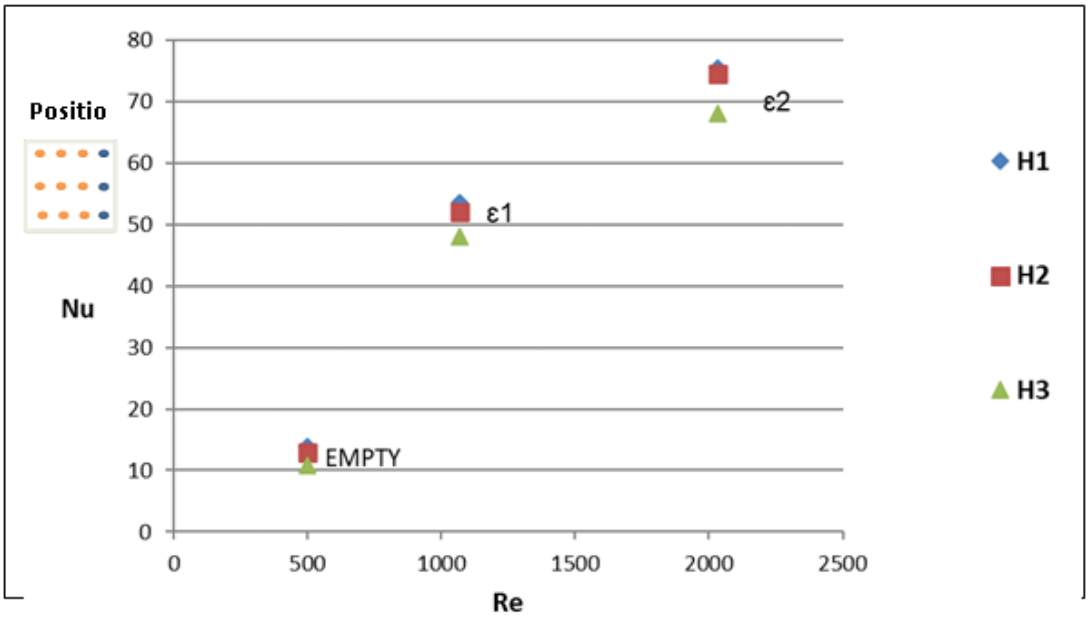

Figure (4–6) shows the relationship between Nu and Re in the P1 & V2

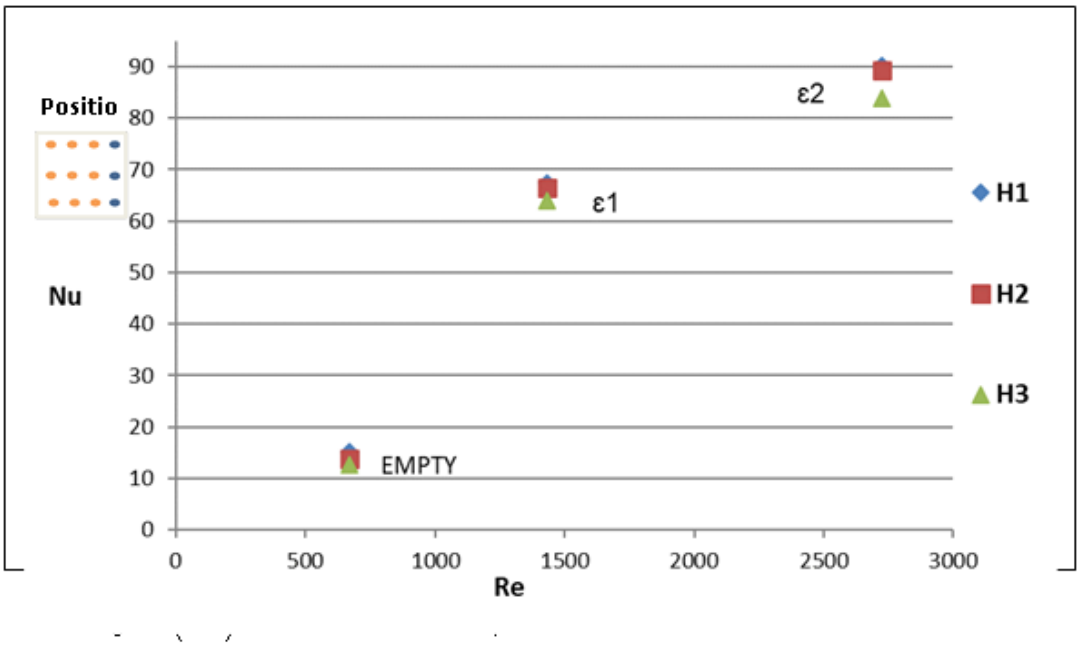

Figure (4-7) shows the relationship between Nu and Re in the P1 & V3

Effect of Nusselt number (Nu) at the angle in different position

The local Nusselt number distribution around heat pipe surface showes a strong dependence on angular position. The highest local Nu values were consistently recorded at the 270° position, corresponding to the stagnation region where the airflow initially impinges on the heat pipe surface. This region experiences higher velocity gradients and stronger convective heat transfer.

Conversely, lower local Nu values were observed at the 90° and 180° positions, where the airflow experiences partial shielding and recirculation effects. These findings confirm that local flow behavior within the porous pad plays a critical role in determining the spatial heat transfer characteristics and should be considered in the design of porous-based heat exchangers figures (4-8) & (4-9) shows effect Nu at angle in deferent position at same velocity and power. Figures (4-10) and (4-11) show the effect of the Nusselt number at the four angles (0°, 90°, 180°, 270°) compared to the Nusselt number on the surface of the convection heaters inside the air pads at positions (3 and 4). In both figures, a first power was used with a third velocity, and the Nusselt number was analysed, showing all different cases (empty) or (ε1, ε2) at the four angles, thus demonstrating the effect of position within the cushion and the extent to which air velocity and heat flux affect the Nusselt number values in the heaters. As analysed in Figures (4-12) in the second power W(150), the extent of its influence at the angle when the speed changes, with the observation of the increased pressure drop, gives the lowest Nusselt number from the surface, especially in porous materials (1ε).

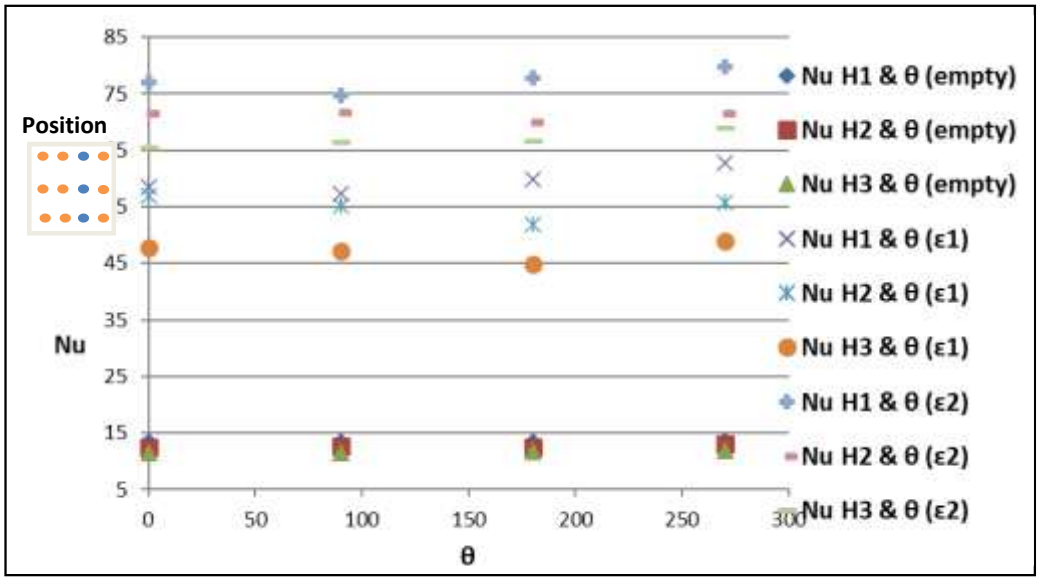

Figure (4-8) illustrates Nusselt number at angles in the case P1 & V1.

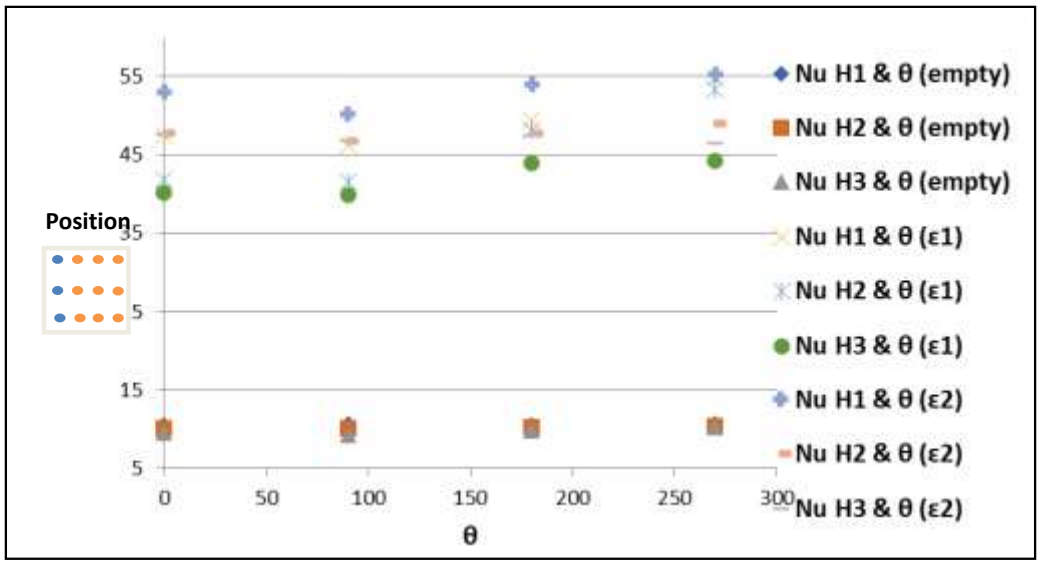

Figure (4-9) illustrates Nusselt number at angles in the case P1 & V1

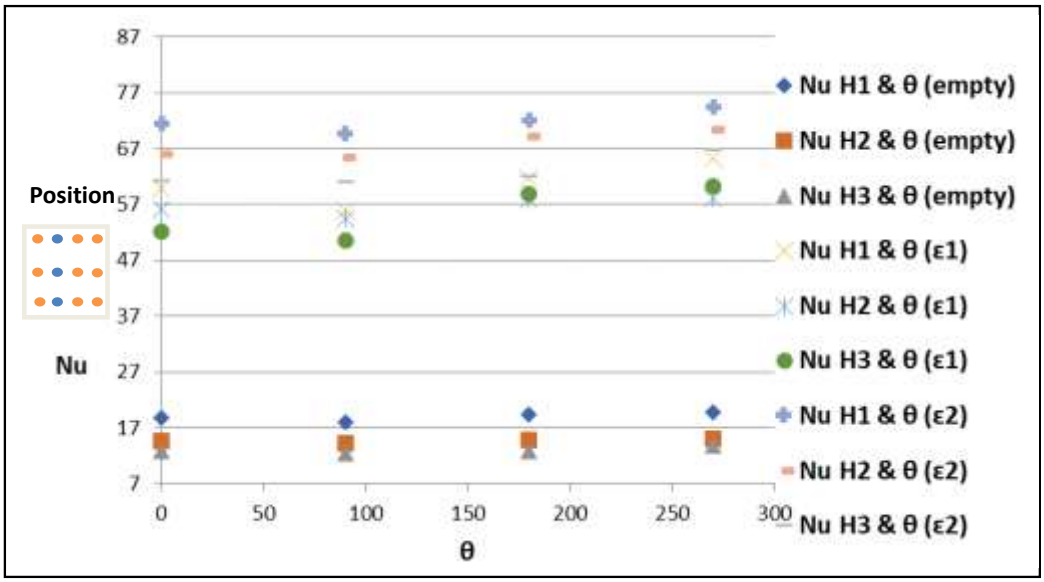

Figure (4-10) illustrates Nusselt number at angles in the case P1 & V3

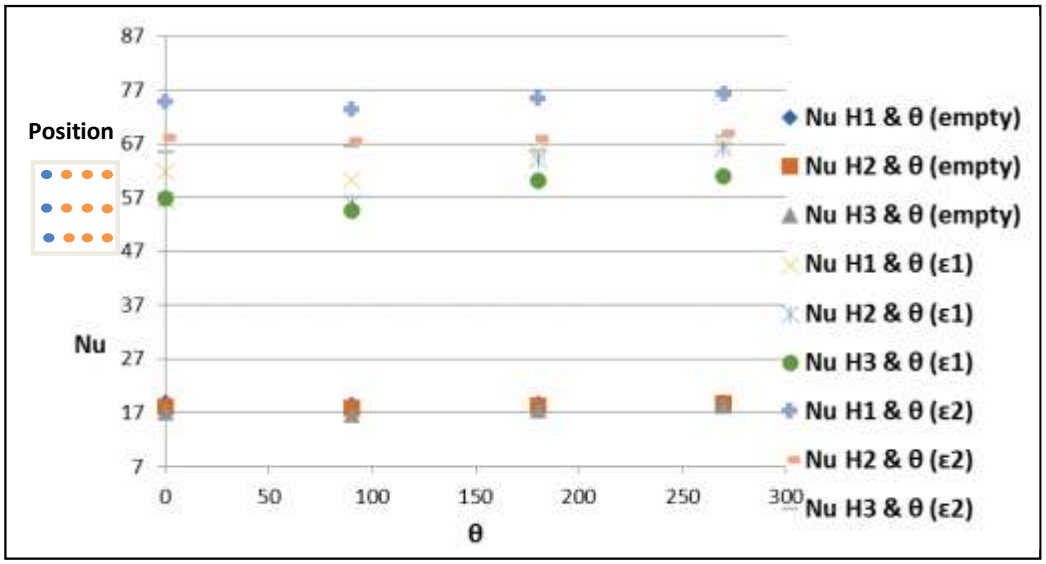

Figure (4-11) illustrates Nusselt number at angles in the case P1 & V3

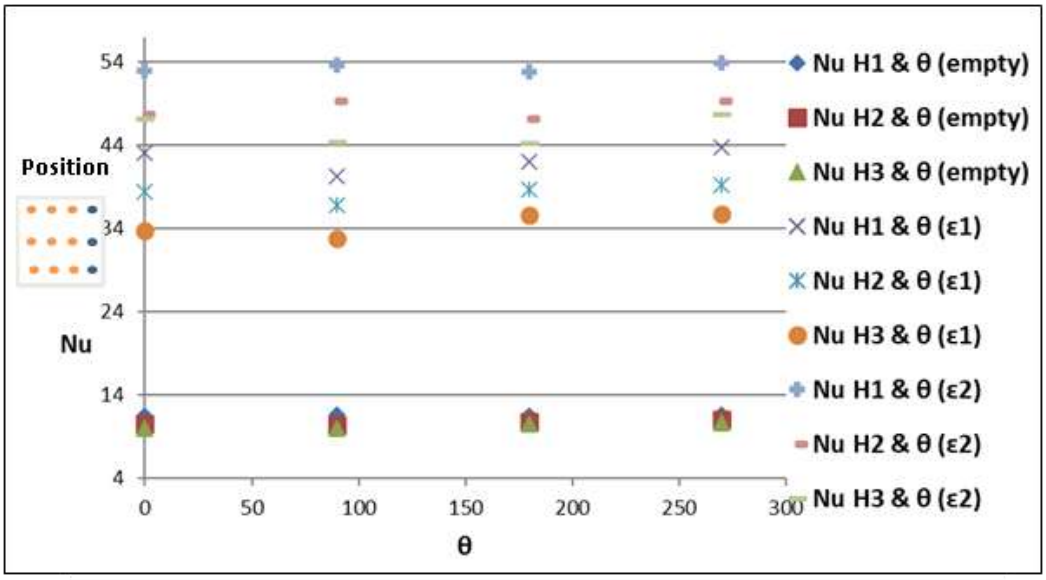

Figure (4-12) illustrates Nusselt number at angles in the case P2 & V1

Relationship between ΔP and Re:

The pressure drop is directly proportional to the Reynolds number; that is, the higher the Reynolds number, the higher the ΔP, thus affecting the cushion's performance. As the porosity of the spheres inside the cushion decreases, the ΔP increases, leading to pressure buildup within the cushion.

When testing the three speeds inside the cushion, it was observed that ΔP increased with increasing speed in all cases. The ΔP inside the cushion was 30 Pa at the first speed (V1), 50 Pa at the second speed (V1), and 80 Pa at the third speed (V3).

However, when using first-degree porosity materials (1ε) with a porosity of (0.53), the results are as follows: at the first velocity (V1) it is (150 Pa), at the second velocity (V1) it is (200 Pa), and at the third velocity (V3) it is (230 Pa). The small size and the spacing between the few spheres led to an increase in ΔP within the cushion, which in turn affected Re and Nu. Note that the lowest Nu was observed at this size, and the increase in ΔP and porosity between a few times led to an increase in conductivity within the cushion as well. When using second-degree porosity materials (2ε) with a porosity of (0.58), the results are as follows: at the first velocity (V1) it is (90 Pa), at the second velocity (V1) it is (140 Pa), and at the third velocity (V3) it is (170 Pa). When tested at the third speed (V3), an increase in Re was observed, causing it to bypass the linear phase and enter the transition phase. This resulted in an effect on Nu and the heat distribution on the heater surface. Figures (4-13) to (4-15) illustrate the relationship between ΔP and Re at different speeds and at different locations within the pad.

Thermo-Hydraulic Performance Considerations

The combined analysis of heat transfer and pressure drop highlights the trade-off inherent in porous media applications. While increasing airflow velocity, reducing particle size, and decreasing porosity enhance heat transfer, they also impose higher hydraulic losses.

The results suggest that medium porosity glass beads offer a favourable compromise between thermal enhancement and pressure drop. This finding is particularly relevant for forced-air heating systems, where fan power consumption and system efficiency are critical design constraints.

Overall, the experimental results confirm that porous glass beads significantly enhance convective heat transfer in air heating ducts, provided that their geometric and operating parameters are carefully optimize.

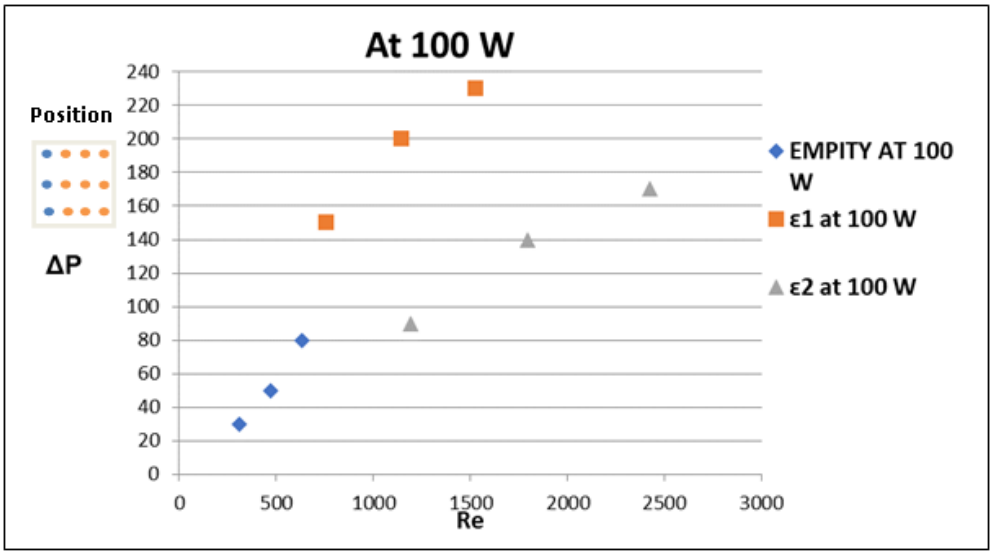

Figure (4-13) shows the relationship between ΔP and Re at (V1, V2, V3) at **P1**

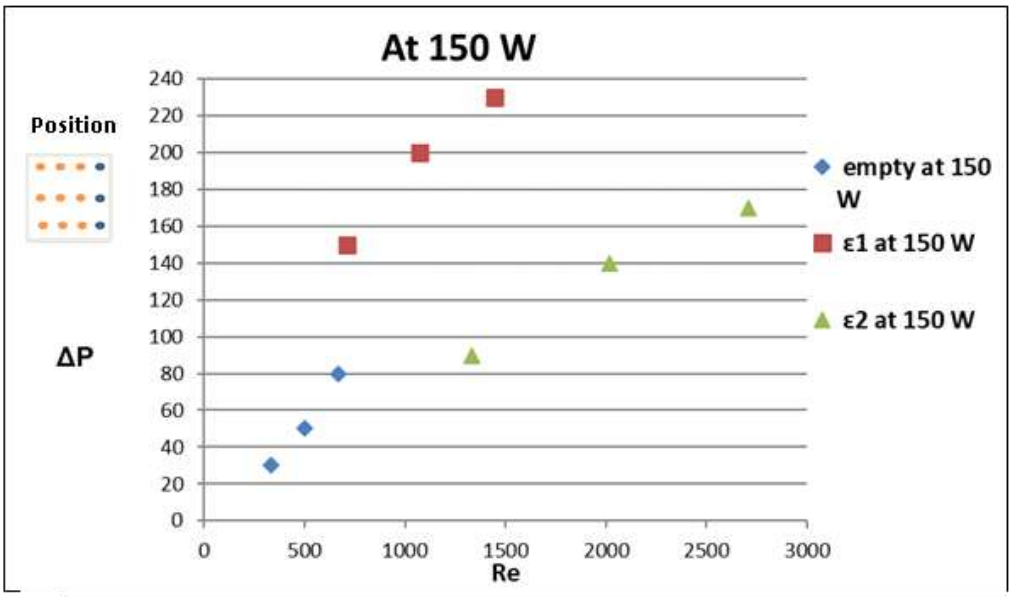

Figure (4-15) shows the relationship between ΔP and Re at (V1, V2, V3) at **P2**

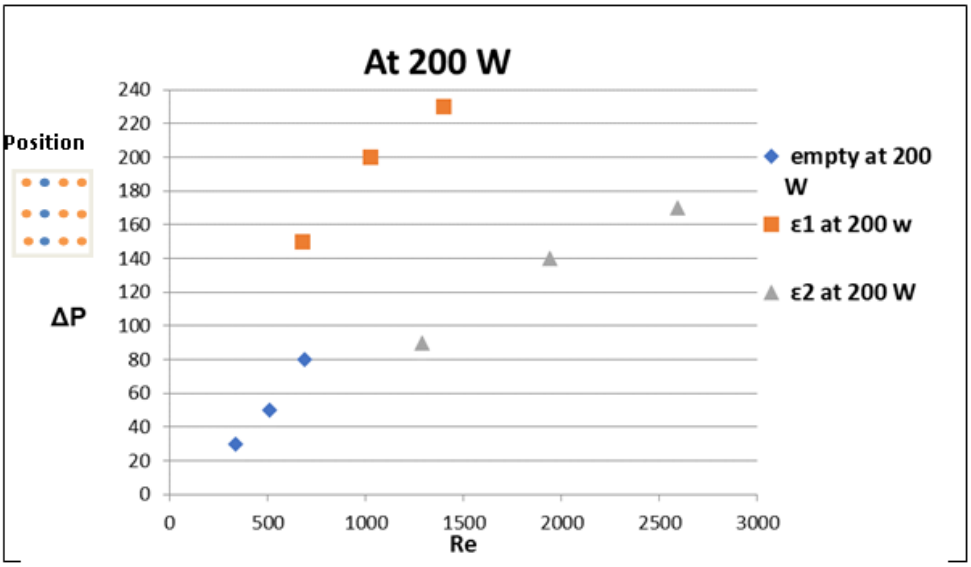

Figure (4–15) shows the relationship between ΔP and Re at (V1, V2, V3) at P3

CONCLUSION

Fundamental Finding : 1) The introduction of porous glass beads significantly enhanced convective heat transfer compared to the non-porous configuration. This was primarily due to increased heat transfer surface area, intensified air–solid interaction, and repeated disruption of the thermal boundary layer within the porous structure. 2) Smaller glass bead diameters led to higher Nusselt numbers, with improvement ratios up to 66.10%, 89.79%, and 64.83% at different heat inputs under identical airflow conditions. 3) Increasing airflow velocity resulted in higher Reynolds and Nusselt numbers, improving convective heat transfer and contributing to a more uniform temperature distribution around the heat pipe. 4) The highest local heat transfer rates were consistently observed at the 270° position due to airflow impingement, while lower values occurred where flow shielding and recirculation were present. 5) Pressure drop across the porous pad increased non-linearly with Reynolds number, especially for lower porosity and smaller bead sizes. 6) A trade-off was identified between heat transfer enhancement and hydraulic penalty, with smaller beads and lower porosity improving heat transfer but causing higher pressure losses. **Implication :** 1) The findings suggest that medium-porosity configurations offer a balanced thermo-hydraulic performance, making them more suitable for practical forced-air heating applications. 2) The study provides valuable insights into the design and optimization of porous-based heat exchangers and air heating ducts, indicating that careful optimization of geometric characteristics and operating conditions can significantly improve thermal performance. **Limitation :** 1) The study only focused on porous glass beads, and the effects of other porous materials, such as metal foams or aluminium beads, were not examined. 2) The study did not consider varying heat flux distributions or include numerical simulations for further validation and generalization of the findings. **Future Research :** 1) Future studies should investigate different porous materials like metal foams or aluminium beads. 2) Further work can

include exploring varying heat flux distributions and incorporating numerical simulations to validate and expand on the current experimental findings.

REFERENCES

[1] F.F. Qader, et al., "Numerical study of heat transfer in circular pipe filled with porous medium," *Pollack Periodica*, vol. 19, no. 1, pp. 137-142, 2024.

[2] B. Zallama, L. Zili Ghedira, and S. Nasrallah, "Forced convection in a cylinder filled with porous medium, including viscous dissipation effects," *Journal of Applied Fluid Mechanics*, vol. 9, Special Issue 1, pp. 139-145, 2016.

[3] S.T.M. Al-Mousawe, et al., "Combined forced and free convection within an enclosure filled with a porous medium," *Journal of Mechanical Engineering Research and Developments*, vol. 44, no. 2, pp. 293-305, 2021.

[4] M.F. Yousif, S.N. Shehab, and H.M. Jaffal, "Experimental Study of Forced Heat Convection through a Vertical Porous Annuli," *Journal of Mechanical Engineering Research and Developments*, vol. 43, no. 2, pp. 116-126, 2020.

[5] K. Leong, et al., "Numerical and experimental study of forced convection in graphite foams of different configurations," *Applied Thermal Engineering*, vol. 30, no. 5, pp. 520-532, 2010.

[6] M.T. Pamuk, "Numerical study of heat transfer in a porous medium of steel balls," *Thermal Science*, vol. 23, no. 1, pp. 271-279, 2019.

[7] H. Aghamiri, M. Niknejadi, and D. Toghraie, "Analysis of the forced convection of two-phase Ferro-nanofluid flow in a completely porous microchannel containing rotating cylinders," *Scientific Reports*, vol. 11, no. 1, p. 17811, 2021.

[8] H.N. Abdulkareem and K.H. Hilal, "Convection heat transfer analysis in a vertical porous tube," *Wasit Journal of Engineering Sciences*, vol. 8, no. 1, pp. 31-45, 2020.

[9] S.A. Rasheed, "Enhancement in Forced Convection Heat Transfer from a Heated Triangular Cylinder by Using Porous Media," *Journal of Mechanical Engineering Research and Developments*, vol. 44, no. 1, pp. 135-150, 2021.

[10] R.G. Saihood and M.F.F. Ala, "Experimental study of partial open side effect on natural convection in a porous cavity," *Journal of Engineering*, vol. 30, no. 06, pp. 172-187, 2024.

[11] M.A. Eleiwi, "Theoretical and Experimental Study of Forced Convection Heat Transfer from a Horizontal Cylinder Embedded in Porous Medium," *Journal of Kirkuk University–Scientific Studies*, vol. 7, no. 2, 2012.

[12] S. Mahgoub, "Forced convection heat transfer over a flat plate in a porous medium," *Ain Shams Engineering Journal*, vol. 4, no. 4, pp. 605-613, 2013.

[13] A. Aamer, "Experimental and Theoretical Study of Forced Convection around a Cylinder Embedded in Porous Media," *The Iraqi Journal for Mechanical and Materials Engineering*, vol. 20, no. 2, pp. 164-179, 2020.

[14] S.A. Ali and S.A. Rasheed, "Investigating heat transfer and turbulent flow in a channel for different cross sections full-filled with glass spheres as a porous media," *Al-Iraqia Journal for Scientific Engineering Research*, vol. 2, no. 1, pp. 13-23, 2023.

[15] P.F. Dickson, *Heat Transfer*, JP Holman, McGraw Hill Book Company, 1977, p. 530.

[16] T. Wang, et al., "Experimental study and theoretical analysis of fluid resistance in porous media of glass spheres," *Chinese Physics B*, vol. 26, no. 7, p. 074701, 2017.

[17] A.H. Darweesh and Z.K. Kadhim, "Influence of the Aspect Ratio on the Free Convection Heat Transmission Properties of a Container Containing Porous Materials," *Journal of Advanced Research in Fluid Mechanics and Thermal Sciences*, vol. 99, pp. 174-195.

[18] S.A. Rasheed and J.M. Abood, "Forced convection heat transfer from a different cross section cylinder embedded in porous media," *Al-Nahrain Journal for Engineering Sciences*, vol. 20, no. 3, pp. 727-736, 2017.

[19] T.A. Tahseen, "An experimental study for mixed convection through a circular tube filled with porous media and fixed horizontally and inclined," *Modern Applied Science*, vol. 5, no. 2, p. 128, 2011.

*** Mohammed Z. Hameed (Corresponding Author)**
Northern Technical University, Iraq
Email: wisal.salem@uobasrah.edu.iq

Musa Mustafa Weis
Northern Technical University, Iraq